

Single Phase Single Stage grid connected PV system

Mukesh Mishra
Swami viveakanad subharti
university,Meerut U.P
(India)

Durgesh kumar
Swami viveakanad subharti
university,
Meerut U.P (India)

Jaysing A. Kshirsagar
Dr. Babasaheb Ambedkar
Technological University
Lonere(India).

Abstract:- The electricity sector have many quandary regarding, the supply of electricity, so renewable energy promotion policies have increase the solar energy consumption. The consequential of photovoltaic cell connected to the grids. These papers propose the single stage inverter with maximum power point tracking (MPPT) and one cycle controlled (OCC) for grid connected PV system. One cycle controlled scheme is predicated on the output current adjustment .Schemes predicated on one-cycle control (OCC) which do not require the accommodation of a phase locked loop for interfacing the inverter to the grid are increasingly being employed for such applications. It requires less no. of sensors (two) as compared to that required (four) in the earlier reported scheme for the implementation of the core controller comprising of OCC and MPPT blocks. The maximum power extracted from the PV array we are Peterman and observation method.

Keywords— One Cycle Control (OCC); Maximum Power Point Tracking (MPPT); Photovoltaic (PV) array; Single phase grid connected inverter.

I. INTRODUCTION

The rapid increase in the industrial area, the fossil fuel consumption is increase day by day. Rapid increase in pollution in the environment it increments in ecumenical warming and damage ecological. Due to these there is need to increment the utilization of renewable energy in the environment, there are many renewable energy in the environment such as wind, tidal solar and etc. Among all these renewable energy solar energy is obtainable yarely so that the ordinant dictation for photovoltaic (PV) panel has been incrementing more and more. The output voltage and current of a PV panel vary with irradiation, panel temperature and power loading nonlinearly. Under certain atmospheric condition, there subsists a maximum power point. To draw maximum power from PV panel, a sizably voluminous number of researchers have proposed maximum power point tracking (MPPT) algorithms such as voltage feedback method [1]. In these papers we are discussing about photovoltaic cell connected to the grid.

A grid connected PV system has become very popular because of their application in distributed generation and for efficaciously utilizing the PV array potency. The symbolic grid –connected system is shown in fig 1.

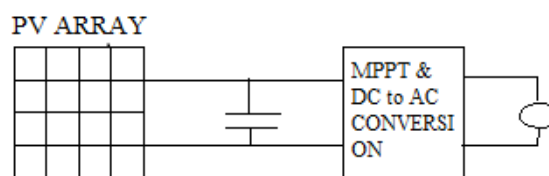


Fig.1 A generic grid connected PV system.

A grid connected PV system has many power processing stages [2], [3].The first stage is dc –dc conversion which extract maximum power by utilizing a maximum power point tracking (MPPT).the second stage is inverting the dc to a A.C conversion and then aliment to the grid .the output of this stage is then inverted by utilizing the inverter. The inverter ascertains that whatever amount of potency is extracted from the solar array is being dumped on the grid which is achieved by maintaining the dc-link voltage at a set reference. Like two stage systems, the single stage inverter performs two functions: 1) obtaining maximum power by utilizing congruous MPPT algorithm .2) these potencies are distributed to the grid by maintaining felicitous power quality discipline of the utility. The grid connected pv system consist of two current control loop, An expeditious inner current controller regulates the current injected to the grid while maintaining prescribed total harmonic distortion (THD) and power factor, while a slow outer current-control loop incorporates the MPPT algorithm employed. When interfacing PV system to grid, it

value of $2V_m$ is engendered utilizing a resettable integrator. A free-running clock having a duration T_s is utilized to reset the integrator, and hence, the frequency of the clock T^{-1} s decides the frequency of the sawtooth waveform as well as the switching frequency of the contrivances. The time constant of the integrator T_i is opted to be a moiety of T_s as expounded in [6]. A fictitious current signal proportional to the fundamental component of the output voltage of the inverter (if = V_{I1}/R_p) is integrated with the source current and opportunely scaled to obtain the modulating signal x , where

$$X = I_S + I_F = I_S + \frac{V_I}{R_p} \quad (2)$$

In order to obtain V_{I1} and hence if, inverter switching pulses are passed through a saturator. The output of the saturator pulsates between the scaled dc-link voltage (V_{dc}) and zero in tandem with the pulsation of the switching sequence between the states one and zero. The signal proportional to V_{I1} is obtained by filtering the output of the saturator. The harmonic spectrum of the saturator output has: 1) a fundamental frequency component (50 Hz); 2) a dc component; and 3) higher frequency components centered around multiples of switching frequency. Hence, a band pass filter (BPF) is required to retrieve the fundamental component of this signal and filter out the dc and higher order components. A second-order BPF having a central frequency identically tantamount to the puissance frequency (50 Hz) is utilized for the purport. The circuit diagram of the second-order filter is shown in Fig. 4. The modulating signal is multiplied by a gain R_s and is then compared with the sawtooth waveform to engender the switching pulses. At every elevating edge of the clock pulse, S3 and S4 are turned on which leads to the increment

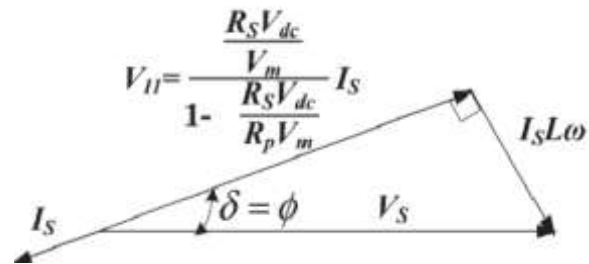


Fig.5-Phasor diagram depicting the steady-state compartment of the proposed voltage-sensor less system.

in source current is. When the modulating signal becomes identically tantamount to the sawtooth waveform, S3 and S4 are turned off and S1 and S2 are turned on so that the modulating signal and hence is decrease. The elevating and falling slopes of i_s are given by $(v_s + V_{dc})/L$ and $(v_s - V_{dc})/L$, respectively, where v_s is utility voltage, V_{dc} is the dc-link capacitor voltage, and L is the magnitude of the boost inductor. The modulating signal x is being compared with the sawtooth waveform to engender the switching pulses. When x is less than the sawtooth waveform, S3 and S4 are on, and the output voltage of the inverter is $-V_{dc}$. When x is more preponderant than the sawtooth waveform, S1 and S2 are turned on, and the output voltage of the inverter is $+V_{dc}$. Hence, the average output voltage of the inverter during a switching duration (time period of the sawtooth waveform) is

$$V_M = \frac{V_M - X}{2V_M} (-V_{dc}) + \frac{V_M + X}{2V_M} (V_{dc}) = \frac{V_{dc}}{V_m} X \quad (3)$$

Therefore, it can be inferred from (3) that the average inverter output voltage in a switching duration is proportional to the modulating signal x . Further, the fundamental component of the output voltage of the inverter will be in phase with the modulating signal. By coalescing (2) and (3), the expression for the inverter output voltage averaged over a switching time period is obtained as follows:

$$V_M = \frac{R_S V_{dc}}{V_M} (I_S + \frac{V_I}{R_p}) \quad (4)$$

From the aforementioned expression, it can be inferred that V_i and i_s are having a phase shift of either 0° or 180° between each other. The phasor diagram exhibiting the grid voltage, the fundamental component of the inverter output voltage, and the drop

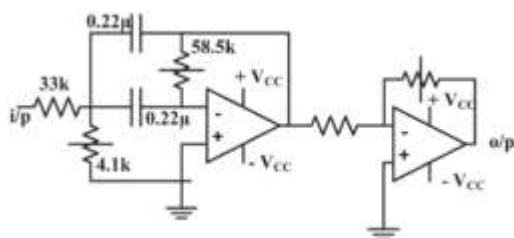


Fig. 4-Circuit diagram of analog implimentaion of BPF

across the series filter inductance is depicted in Fig. 5 for the inverting mode of operation.

III. MPPT IMPLEMENTATION USING P&O METHOD

P&O method is one of the popular methods to track the maximum-power point [10]. Implementation of MPPT by P&O method is generally done by utilizing DSP or microcomputer, but discrete analog and digital

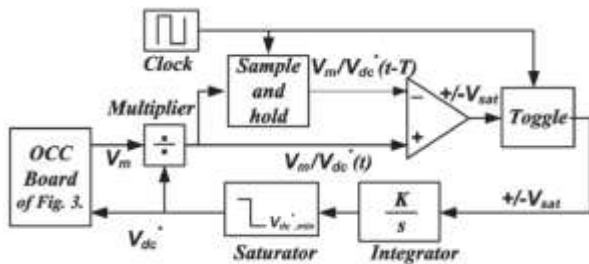


Fig. 5. block diagram of mppt realization

circuitry can withal be utilized for the purport [11]. The analog controller proposed in this paper for the implementation of the P&O algorithm is shown in Fig. 8. The controller consists of an analog multiplier, a sample and- hold circuit, a free-running clock, a toggle switch, and an integrator. The P&O controller receives the signal V_m from the OCC controller of Fig. 3. The output of the P&O controller is V_{dc}^* which sets dc-link voltage reference required by the OCC controller of Fig. 3. An integrator connected to the output of a toggle flip-flop engenders the voltage reference V_{dc}^* . The period of the P&O cycle is decided by a free-running clock which sets sampling instants for the sample-and-hold circuit and toggling instants for the toggle flip-flop. In order to understand the working of the MPPT controller, the typical variations of the different signals of the MPPT controller block are shown in Fig. 9. Depending on the output level of the toggle flip-flop, V_{dc}^* can have either a elevating or a falling slope. The rate of vicissitude in V_{dc}^* is kept much more minute than the control bandwidth of the OCC controller. An analog multiplier of low bandwidth

IV. SIMULATION AND EXPERIMENTAL RESULTS

Simulated Performance

In order to prognosticate the performance of the proposed one cycle-controlled voltage-sensorless grid-connected system, detailed simulation studies are carried out on MATLAB– Simulink platform. In order to objectively show that the proposed voltage sensorless scheme does not have the quandary of current instability while operating in the inverting mode of operation, a model of the system shown in Fig. 1 is simulated [12]. The parameters the inverter culled for the purport of simulation [12] and the controller are as follows:

- 1) switching frequency: 20 kHz;
- 2) dc-link capacitor: 2200 μ F;
- 3) series inductor: 2 mH;
- 4) R_p : 1.5 Ω

The designations for the solar array utilized in the simulation study are provided in Table I, corresponding to 1000W/m² and 800W/m² insolation levels. The dc-link reference is externally set at 220 V. The grid considered as a 230 Vrms 50-Hz system.

Table I

PV ARRAY SPECIFICATIONS

Peak power(P_p)	2KW	1.5KW
Peak power	220V	188V
voltage(V_{MP})	8.8A	6A
Current at peak power (I_{mp})	230V	195V
Open circuit voltage(V_{OC})	1000W/M ²	800W/M ²
Solar iosaltion		

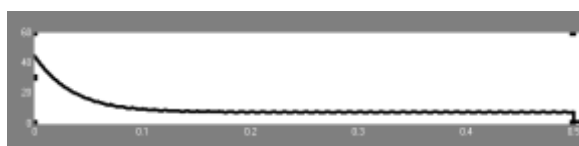
When isolation level abruptly transmuted from 1000W/m² to 800W/m². The DC link voltage is suddenly fall at 188V and current is transmuted from 8.8A to 6A. And maximum power output of PV array is transmuted from 2kw to 1.5kw at 3 sec. After 8 sec, the voltage, current, power is settle back to the initial value. When isolation level abruptly transmuted from

1000W/m² to 800W/m². The DC link voltage is suddenly fall at 188V and current is transmuted from 8.8A to 6A. And maximum power output of PV array is transmuted from 2kw to 1.5kw at 3Sec. After 8 sec, the voltage, current, power is settle back to the initial value. Fig. (5) Shows the Simulation results such as waveforms of the DC link voltage, Grid current, and Grid voltage abruptly transmuted from 1000W/m² to 800W/m². The DC link voltage is suddenly fall at 188V and current is transmuted from 8.8A to 6A. And maximum power output of PV array is transmuted from 2kw to 1.5kw at 3 sec.

Dc link voltage



Dc link current



Grid voltage

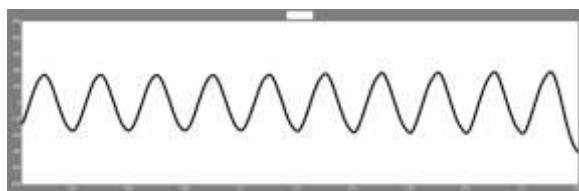


Fig. show the a)dc link voltage b)dc link current c)grid voltage.

From the simulated performance, it can be inferred that the system supplies the available maximum power from the PV array to the grid. The transient performance of the system can be optically discerned during the vicissitude in insolation levels. Moreover, it can be observed from the simulated performance that the vicissitudes in PV current and dc-link voltage are smooth during the transmuted in insolation level which implicatively insinuates a copacetic transient performance for the system. The steady-state grid voltage, source current, dc-link voltage, and the fictitious current signal obtained from the filtered

output of the switching pulses of the inverter are shown in Fig. 5. It can be noted that the grid voltage and source current are virtually 180° out of phase thereby demonstrating the inverting mode of operation. The quantified harmonic spectrum of the current supplied by the system to the grid and the grid voltage from which it can be inferred that all the low order harmonics to that of the fundamental component. As an OCC-predicated scheme poses itself as equipollent impedance to the grid, distortions present in the grid voltage withal appear in the current drawn by the system from the grid.

V. CONCLUSION

An M-OCC predicated Single phase Single stage voltage preposterous grid connected PV system has been proposed. The circumscription of the subsisting OCC predicated inverters, such as requisite for sensing the grid voltage to tackle the instability quandary, is circumvented in the proposed scheme. The proposed scheme is predicated on a single stage of potency conversion and is realized by utilizing a considerably less number of sensors compared to that of conventional schemes. Further, the core controller of the proposed scheme can be realized by designates of a very simple analog controller. All the aforementioned features of the scheme make it an ideal candidate for minuscule and distributed single-phase grid connected PV systems. Detailed simulation studies have been carried out to verify the efficacy of the scheme. The viability of the scheme has been corroborated by performing detailed simulation studies.

REFERANCE

- [1] Z. Salameh, F. Dagher and W.A. Lynch, "Step-Down Maximum Power Point Tracker for Photovoltaic System," *Solar Energy*, vol. 46, no. 1, 1991, pp. 278-282.
- [2] M. Calais, J. Myrzik, T. Spooner, and V. Agelidis, "Inverters for single phase grid connected photovoltaic systems—An overview," in *Proc. IEEE Power Electron. Spec. Conf.*, Jun. 2002, pp. 1995–2000.
- [3] S. B. Kjaer, J. K. Pedersen, and F. Blaabjerg, "Power inverter topologies for photovoltaic modules—A review," in *Conf. Rec. IEEE IAS Annu. Meeting, 2002*, vol. 2, pp. 782–788.
- [4] Dezso Sera, Laszlo Mathe, Tamas Kerekes, Sergiu Viorel Spataru, and Remus Teodorescu, "On the Perturb-and-Observe and Incremental Conductance MPPT Methods for PV Systems" *ieee journal of photovoltaics*, vol. 3, no. 3, july 2013.

-
- [5] Q. Chongming and K. M. Smedley, “Unified constant-frequency integration control of three-phase standard bridge boost rectifiers with power factor correction,” *IEEE Trans. Ind. Electron.*, vol. 50, no. 1, pp. 100–107, Feb. 2003.
 - [6] K. M. Smedley, L. Zhou, and C. Qiao, “Unified constant-frequency integration control of active power filters—Steady-state and dynamics,” *IEEE Trans. Power Electron.*, vol. 16, no. 3, pp. 428–436, May 2001.
 - [7] K. Chatterjee, D. V. Ghodke, A. Chandra, and K. Al-Haddad, “Simple controller for STATCOM-based var generators,” *IET Power Electron.*, vol. 2, no. 2, pp. 192–202, Mar. 2009
 - [8] D. V. Ghodke, K. Chatterjee, and B. G. Fernandes, “Modified one cycle controlled bi-directional high power factor AC to DC converter,” *IEEE Trans. Ind. Electron.*, vol. 55, no. 6, pp. 2459–2472, Jun. 2008.
 - [9] D. V. Ghodke, E. S. Sreeraj, K. Chatterjee, and B. G. Fernandes, “One cycle controlled bi-directional AC to DC converter having constant power factor operation,” *IEEE Trans. Ind. Electron.*, vol. 56, no. 5, pp. 1499–1510, May 2009.
 - [10] B. K. Bose, P. M. Szesesny, and R. L. Steigerwald, “Microcontroller control of residential photovoltaic power conditioning system,” *IEEE Trans. Ind. Appl.*, vol. 21, no. 5, pp. 1182–1191, Sep. 1985.
 - [11] G. Petrone, G. Spagnuolo, R. Teodorescu, M. Veerachary, and M. Vitelli, “Reliability issues in photovoltaic power processing systems,” *IEEE Trans. Ind. Electron.*, vol. 55, no. 7, pp. 2569–2580, Jul. 2008
 - [12] Sreeraj E. S., Kishore Chatterjee, and Santanu Bandyopadhyay, “One-Cycle-Controlled Single-Stage Single-Phase Voltage-Sensorless Grid-Connected PV System,” *IEEE transactions on industrial electronics*, VOL. 60, NO. 3, MARCH 2013.